Genome-Wide Screening of Aberrant Methylation Loci for Nonsyndromic Cleft Lip

Xiao-Yan Xu, Xiao-Wei Wei, Wei Ma, Hui Gu, Dan Liu, Zheng-Wei Yuan

Key Laboratory of Health Ministry for Congenital Malformation, Shengjing Hospital, China Medical University, Shenyang, Liaoning 110004, China

Abstract

Background: The pathogenicity of cleft lip (CL) is pretty complicated since it is influenced by the interaction of environment and genetic factors. The purpose of this study was to conduct a genome-wide screening of aberrant methylation loci in partial lesion tissues of patients with nonsyndromic CL (NSCL) and preliminarily validate candidate dysmethylated genes associated with NSCL.

Methods: Fifteen healthy and sixteen NSCL fetal lip tissue samples were collected. The Infinium HumanMethylation450 BeadChip was used to screen aberrant methylation loci in three NSCL and three healthy lip tissues. The differential methylation sites and functions of the annotated genes between NSCL and healthy lip tissues were analyzed using minfi package of R software, cluster analysis, Gene Ontology (GO) annotation, and metabolic pathway annotation. Gene expression was assessed in nine differentially methylated genes by real-time polymerase chain reaction (PCR). The transcriptions mRNA levels of three out of nine candidate genes were downregulated remarkably in NSCL lip tissues, and these three genes' abnormal methylation loci were validated by pyrosequencing in 16 NSCL cases and 15 healthy cases.

Results: In total, 4879 sites in the genes of NSCL odinopoeia fetuses showed aberrant methylation when compared with normal lip tissue genome. Among these, 3661 sites were hypermethylated and 1218 sites were hypomethylated as compared to methylation levels in healthy specimens. These aberrant methylation sites involved 2849 genes and were widely distributed among the chromosomes. Most differentially methylated sites were located in cytosine-phosphoric acid-guanine islands. Based on GO analysis, aberrantly methylated genes were involved in 11 cellular components, 13 molecular functions, and a variety of biological processes. Notably, the transcription of *DAB1*, *REELIN*, and *FYN* was significantly downregulated in lesion tissues of NSCL fetus ($P < 0.05$). Pyrosequencing results validated that there were two loci in *DAB1* with high methylation status in patient tissues ($P < 0.05$).

Conclusions: We detected numerous aberrantly methylated loci in lesion tissues of NSCL fetus. Aberrant gene expression in the *REELIN* signaling pathway might be related with NSCL. Decreased transcription of *DAB1*, a member of *REELIN* signal pathway, resulted from its abnormal high methylation, which might be one of the factors underlying the occurrence of NSCL.

Key words: *DAB1*; Methylation; Nonsyndromic Cleft Lip; REELIN Signaling Pathway

INTRODUCTION

Orofacial clefting, which includes cleft lip (CL), CL and palate (CL/P), and cleft palate only (CPO), is a common congenital malformation that has an incidence of 1/700 in newborns.[1,2] During human gestation, the upper lip and palate are derived from the first branchial arch. The maxillary process (MxP) of the first branchial arch and the medial nasal process (MNP) gradually develop closely to fuse and form the upper lip in the 4th week.[3] The oral part of the MxP continues to develop to form the secondary palate and oral cavity.[4] Accumulating evidence indicates that a variety of environmental and genetic factors can harmfully affect lip or palate formation, resulting in CL or CL/P.[5-9] Whether accompanied by other abnormalities or not, orofacial clefting can be divided into syndromic CL (SCL with or without a cleft palate) and nonsyndromic CL (NSCL; with

Access this article online

Quick Response Code:

Website:
www.cmj.org

DOI:
10.4103/0366-6999.239305

or without a cleft palate [NSCL/P]), accounting for 30% and 70% of the total CL cases, respectively.[10] Undoubtedly, orofacial clefting is a complicated polygenic disease, and its exact etiology remains elusive. It is very important to investigate its pathogenesis, particularly pathogenic site or the genes causing this anomaly, as well as early diagnosis and intervention methods. At present, no specific genetic factors, such as gene mutations, contributing to NSCL have been found. Therefore, epigenetic changes (environmental factors) may be a leading cause of NSCL.

In vertebrates, DNA methylation is a key epigenetic modification that plays an important role in a wide range of developmental and disease processes.[11] During embryogenesis, three active DNA methyltransferases, including DNMT-1, DNMT-3a, and DNMT-3b, primarily catalyze mammalian DNA methylation. Abnormal DNA methylation levels via targeted disruption of these genes results in dysmorphologies and even embryonic lethality.[12,13] Specifically, DNMT3b mutation is involved in the occurrence of instability-facial anomalies.[14,15] In addition, the inhibition of DNA methylation by 5-azacytidine exposure *in utero* leads to CP in fetuses.[16] It has been reported that epigenetic control by imprinting could contribute to oral and craniofacial diseases.[17] Even with the active investigation of genetic associations in NSCL and NSCL/P, direct evidence of epigenetic control in candidate regions and at the genome-wide level remains unreported.

The Infinium HumanMethylation450 BeadChip array has been widely used to study DNA methylation in human tissues.[11] To the best of our knowledge, there is no report on DNA methylation in local lesions of patients with NSCL. In addition, the scarcity of NSCL local lesion samples impedes the research in this field. In the present study, we used the Methylation450 BeadChip array to screen aberrant methylation loci in local lesion of NSCL. Reverse transcription-polymerase chain reaction (RT-PCR) was utilized to evaluate aberrant gene expression of the lesion tissues. Selected differentially methylated genes in the REELIN signaling pathway were validated by pyrosequencing in a larger cohort. Finally, we provided evidence that the highly methylated REELIN signaling pathway is potentially functionally associated with NSCL.

METHODS

Ethics approval
There are no ethical/legal conflicts involved in the paper. In this study, all fetus samples were collected from puerperal fetuses discarded at the hospital. This study was approved by the research ethics committee of the hospital (approval No. 2018PS12). Written consent was obtained from each parent before pregnancy termination.

Sample collection
NSCL tissue samples were collected from elective terminations after being diagnosed with NSCL at the Prenatal Diagnosis Center of the Shengjing Hospital of China Medical University. All NSCL fetuses were within the gestational age of 22–30 weeks. Exclusion criteria included fetuses with brain abnormalities, chromosomal abnormalities, or grossly abnormal fetuses. A total of 15 healthy tissue samples were obtained from pregnancy terminations due to unplanned pregnancy and 16 NSCL samples were collected for this study. Mean ± standard deviation (SD) of the gestational age of NSCL fetus is 175.06 ± 23.93 days. That of healthy fetus is 180.07 ± 18.18 days. There is no statistical difference between the two groups ($t = 0.652$, $P = 0.519$).

Methylation chip
Healthy lip and CL samples for the genome-wide methylation screening were obtained from three NSCL fetuses and three healthy fetuses with matched gestation periods. Mean ± SD of the gestational age of NSCL fetus is 179.00 ± 26.23 days. That of healthy fetus is 178.67 ± 30.01 days. There is no statistical difference between the two groups ($t = 0.014$, $P = 0.989$). Genomic DNA was extracted and bisulfite-converted according to a previous report.[18] The Infinium HumanMethylation450 BeadChip (Illumina Inc., San Diego, CA, USA) was used to screen the genome-wide aberrantly methylated loci in NSCL.[18,19] The Methylation450 BeadChip technology has been widely used to detect aberrant gene methylation in some common multigene diseases. Twelve samples can be analyzed on one chip. The chip includes over 450,000 cytosine-phosphoric acid-guanine (CpG) sites throughout the genome, which cover 96% of the CpG islands and 99% of RefSeq genes, as well as non-CpG methylation sites in human stem cells and differential methylation sites between various normal tissues and cancers. In addition, the 450 k array covers some CpG islands in the noncoding, promoter, and disease-associated regions as confirmed by genome-wide association study (GWAS) screening. The accessory Illumina Genome Studio Software (Illumina Inc., San Diego, CA, USA) was used to read the raw intensity, and signal was normalized to the background signal.

Bioinformatics analyses
Differential methylation sites between NSCL and healthy lip tissues and functional gene annotations were analyzed using minfi package of R software (Auckland University, New Zealand), cluster analysis, Gene Ontology (GO) annotation, and metabolic pathway annotation. A linear model was fit to *M* values to assess differential methylation on a per CpG-level, and the gene name was annotated to each 450 k CpG site for gene-based analysis, according to a previous report.[19]

Quantitative reverse transcription-polymerase chain reaction analysis of candidate genes associated with nonsyndromic cleft lip
A large number of aberrant methylation sites in NSCL were obtained from the microarray screening. Candidate genes mapped by biologically relevant candidate CpG sites were selected according to the following two criteria: (1) those reported to be associated with NSCL based on

previous studies, which had significantly high methylation in NSCL ($P < 0.05$, |beta.difference| > 0.14); (2) those with transcription factors involved in important signaling pathways of cellular functions among differentially methylated annotated genes.

The mRNA levels of selected candidate genes were assessed by quantitative reverse transcription-polymerase chain reaction (RT-qPCR) analysis. Total RNA was extracted from each tissue with Trizol Reagent (Invitrogen, Carlsbad, CA, USA). cDNA was prepared from 1 µg of RNA using a Revert Aid™ First Strand cDNA Synthesis Kit (TaKaRa Bio, Japan) and diluted 20-fold in water. SYBR Green was used for quantitative PCRs, which were carried out in triplicate. Differences among target gene expression levels were estimated using the ΔΔCT method and were normalized to the level glyceraldehyde-3-phosphate dehydrogenase mRNA. The data are presented as the mean ± SD. The primers used for RT-qPCR are listed in Table 1.

Validation of the DNA methylation of candidate genes

The differential DNA methylation of candidate genes was validated in 16 NSCL and 15 healthy lip tissue samples by pyrosequencing. Genomic DNA was extracted and bisulfite-converted using an EpiTect Plus DNA Bisulfite Kit (Cat No. 59104, Qiagen, Germany) and EpiTect Bisulfite Kit (Qiagen), following manufacturer's protocols. PCR was performed using the conversed DNA samples as templates.

Table 1: Primers for real-time quantitative PCR in 16 NSCL samples and 15 healthy samples

Gene name	Primer sequence	Product length (bp)
DAB1	F: 5' GGGTTGGAGGTGAGTTGG3'	98
	R: 5'GGCACAGGATACAGACGA3'	
FYN	F: 5' GTCATCTTCTGTCCGTGCT3'	159
	R: 5'CCCAACTACAACAACTTCC3'	
REELIN	F: 5' ATTGGTCCTGTTTGTCTCC 3'	177
	R: 5'CTCCTGGTCCCTCCTTCAC3'	
GAPDH	F: 5' GCACCGTCAAGGCTGAGAAC3'	137
	R: 5'TGGTGAAGACGCCAGTGGA 3'	
MSX1	F: CTCGGACATTTCTCGGTGGG	184
	R: GCGGCTTACGGTTCGTCTTGT	
BMP7	F: TCAAACACCAGCCAGCCCTC	245
	R: TTCTTCCACCCACGCTACCA	
EGFR	F: AGGGCAATGAGGACATAACCAG	186
	R: CCAAGGCACGAGTAACAAGC	
PAX9	F: CCTTCTCCAACCCGTTCACC	136
	R: CTGGGCATCCGCTCCATCAC	
GLI2	F: TATGGAATGGTGGCAAGAG	194
	R: ACGATGAGCGGCTGAGAT	
IRF6	F: TCCTTGGTGCCATCATACA	207
	R: TAAACGCTTCCAGATTCCC	

PCR: Polymerase chain reaction; NSCL: Nonsyndromic cleft lip; *DAB1*: Disabled 1 gene; *GAPDH*: Glyceraldehyde-3-phosphate dehydrogenase; *MSX1*: Muscle segment homeobox 1; *BMP7*: Bone morphogenetic protein; *EGFR*: Epidermal growth factor receptor; *PAX9*: Paired box gene 9; *GLI2*: Glioma-associated oncogene homologue 2; *IRF6*: Interferon regulatory factor 6; *FYN*: Tyrosine protein kinase fyn.

Ten microliters of PCR products were analyzed on the PyroMark Q96 instrument (Qiagen). The primers used for pyrosequencing are listed in Table 2.

Statistical analysis

All analyses were performed on SPSS Statistical Software version 21.0 (IBM SPSS Inc., Chicago, IL, USA). All data for continuous variables in this study had normal distributions and were expressed as mean ± SD. Differences were assessed using analysis of independent-samples *t*-test when NSCL and healthy groups were compared. The differences were considered statistically significant if $P < 0.05$.

RESULTS

Distinctively aberrant methylation levels in nonsyndromic cleft lip

Methylation levels were compared between three NSCL and three healthy lip tissue samples on the basis of a heat map generated by unsupervised hierarchical clustering [Figure 1a]. As shown in Figure 1a, based on the methylation level, the samples were clearly segregated into NSCL and healthy groups, indicating that there was a significant difference in methylation profiles between both groups. There was no significant difference in gestation between the NSCL and healthy groups ($P = 0.989$). Thus, the distinctively aberrant methylation level in NSCL was not attributed to different gestational ages, but was likely associated with NSCL.

Differentially methylated loci between nonsyndromic cleft lip patients and healthy controls

Next, a pooled *t*-test was used to screen differential methylation sites between the NSCL and healthy groups. A total of 4879 sites in the genes were differentially methylated in the NSCL odinopoeia fetuses as compared with normal tissues. Among these, 3661 were hypermethylated and 1218 were hypomethylated as compared with the normal tissues. These differential methylation sites were classified on the basis of gene annotation and CpG island site, as shown in Figure 1b. The aberrant methylation sites were mapped to 2849 genes. Most of the differential methylation sites were located in CpG islands, while others were in CpG shores. Based on the gene annotation classification, differential methylation sites were mostly distributed in the gene body region, followed by transcription start site (TSS1500 region). The black circle indicates the methylation sites and the white circle indicates the nonmethylation sites. The histogram represents the number of differential methylation sites in different locations. As shown in Figure 1c, differential methylation sites were located in all chromosomes, except the Y chromosome.

Functional prediction of genes differentially methylated in nonsyndromic cleft lip

The 2849 aberrantly methylated genes in NSCL were functionally annotated by GO analysis (http://www.geneontology.org) and mapped to signaling pathways and processes [Figure 2]. The relationships between differential methylation sites and their functional annotations were

Gene	Primers	Sequences
DAB1	cg01055518-F	5'AAGGAGTTTTGATTTTTGTGTGTTA3'
	cg01055518-R	5'CCTCCTACATAACCATAAACAAATTACTT3'
	cg01055518-S	5'AGTTTTAGTAGGTAGGTG3'
DAB1	cg01771213-F	5'TTTTTTTAGGGTGAAAGGTAAAGG3'
	cg01771213-R	5'CCCAACATAAACTCAAAACTCACTAA3'
	cg01771213-S	5'CTTAAAAAACTCAAACAATAACCA3'
DAB1	cg13060236-F	5'AGAGATTGTAGGGAGAATTTAATTTG3'
	cg13060236-R	5'AAAACCATCTCCACTCTTTTCTTTACAATA3'
	cg13060236-S	5'TGTAGGGAGAATTTAATTTGA3'
FYN	cg08926365-F	5'AGAAAAGAGGTGGAAGTTTAGAGTT3'
	cg08926365-R	5'AAAACTTACCCCACAAAATACCCTACC3'
	cg08926365-S	5'GGGAAGTTTGATTATAAGTAG3'
FYN	cg12059864-F	5'AAGAGAGGTAGGGTGTTTATGA3'
	cg12059864-R	5'CTACAAAATTTCTCTTAACCAACATATCT3'
	cg12059864-S	5'GTGTTTATGAGGAAGGT3'

NSCL: Nonsyndromic cleft lip; *DAB1*: Disabled 1 gene; *FYN*: Tyrosine protein kinase fyn.
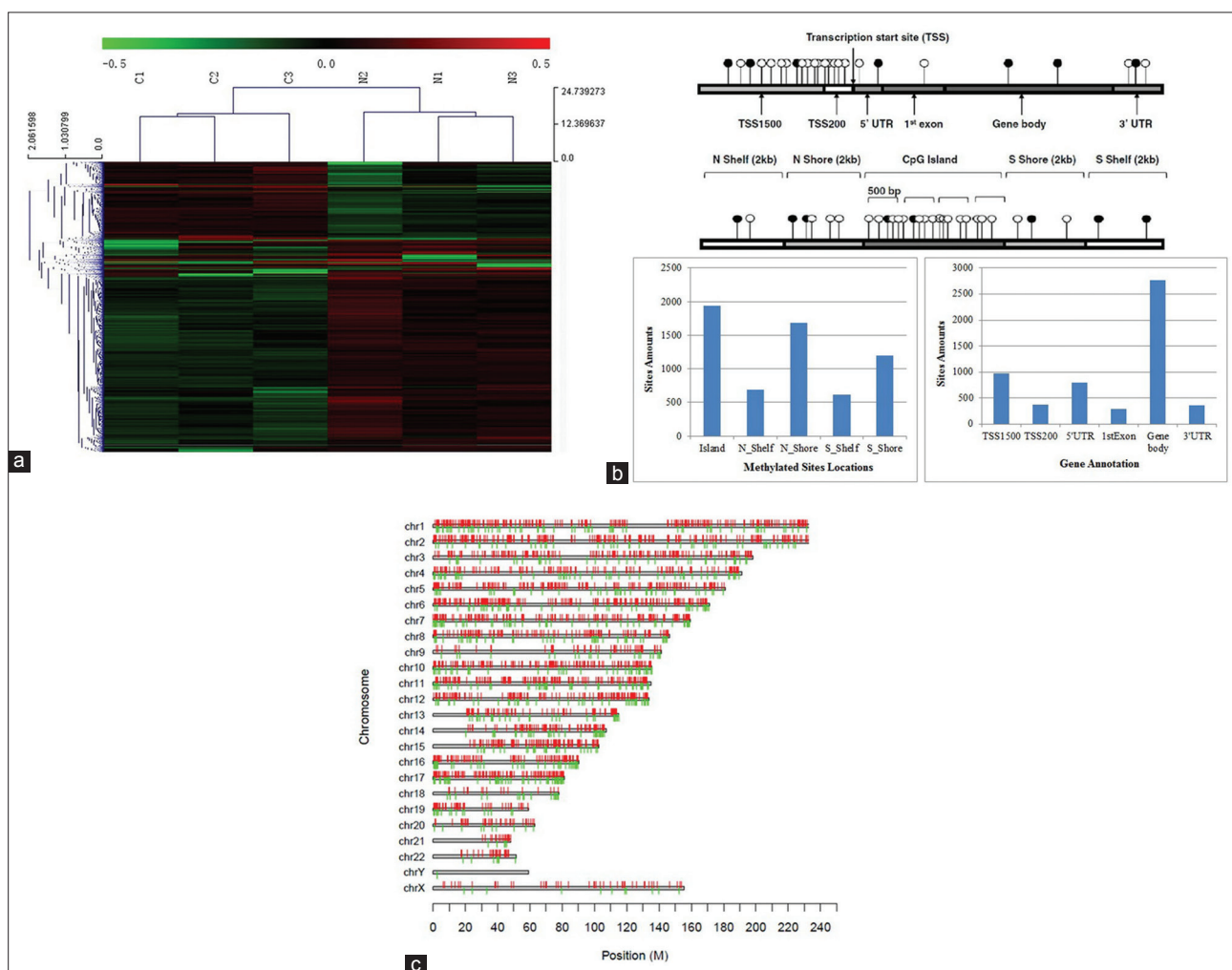

Figure 1: Aberrant methylation levels in NSCL. (a) Heat map based on unsupervised hierarchical clustering; samples are clearly segregated into NSCL and healthy groups. (b) Differentially methylated sites classified according to gene annotation and CpG island site, respectively. The black circle indicates the methylation sites and the white circle indicates the nonmethylation sites. The left lower histogram showed differentially methylated sites distribution at the different locations in CpG island. The right lower histogram showed differentially methylated sites distribution of different gene annotation. (c) Differentially methylated sites are widely distributed on all chromosomes, except the Y chromosome. The red color and green color represents the high- and low-methylation sites in the experimental group, respectively. Gray color represents no difference in methylation among groups. CpG: Cytosine-phosphoric acid-guanine; NSCL: Nonsyndromic cleft lip.
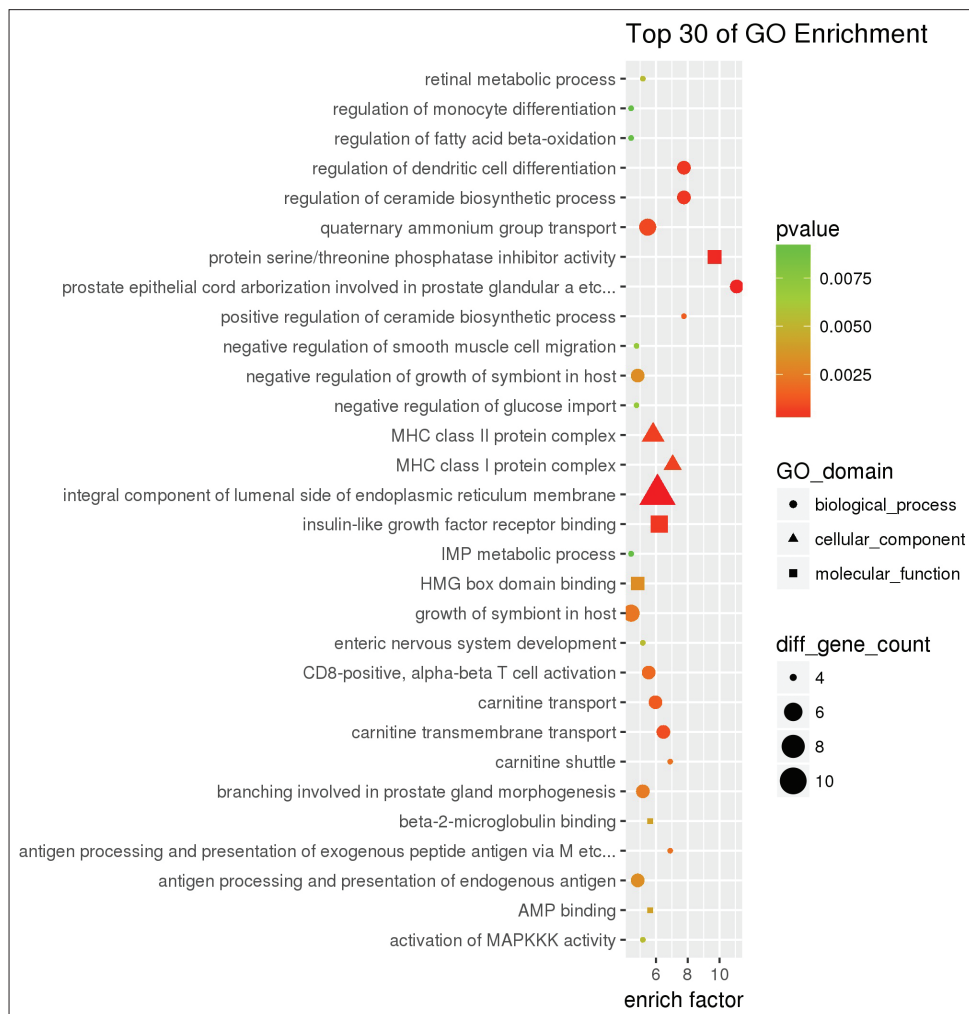
Figure 2: Functional prediction of aberrantly methylated genes by GO annotation analysis. GO: Gene ontology; MHC: Major histocompatibility complex; IMP: Inosine monophosphate; HMG: Human menopausal gonadotropin; CD8: Cluster of differentiation 8; AMP: ADENOSINE monophosphate; MAPKKK: Mitogen-activated protein kinase kinase.

predicted through GO pathway annotations, and sorted by *q*-value, frequency counting, and statistical function annotation, according to biological process, cellular component, and molecular function, respectively.

The 30 GO terms linked with the most differentially methylated sited involved 22 biological processes, three cellular components, and five molecular functions. As for biological processes, signal transduction and signal regulation were the most prominent classes. Predicted cellular components were mainly involved in organelle functions and cell membrane structure. Predicted molecular functions primarily included the transcription factor-binding domain, protein receptor, and protein kinase activation.

mRNA expression of candidate genes as assessed by quantitative reverse transcription-polymerase chain reaction

Nine candidate genes that showed abnormally high methylation were tested by RT-qPCR in 16 lesions and 15 control tissues to examine their mRNA expression

levels. As shown in Figure 3, the results showed that the mRNA expression of *DAB1*, *FYN*, and *REELIN* was significantly ($P < 0.05$) decreased, while that of *MSX1*, *GLI2*, and IRF6 gene was significantly ($P < 0.05$) increased in the NSCL as compared to healthy tissues. No differential mRNA expression was observed for *BMP7*, *EGFR*, and *PAX9* between both tissues.

Validation of Illumina chip data by pyrosequencing

We validated the Illumina chip data for *DAB1* and *FYN*, which showed a significant decrease in methylation in NSCL samples, by pyrosequencing in the 16 lesion and 15 control tissue samples. As shown in Figure 4, the pyrosequencing result confirmed the significantly lower methylation level ($P < 0.05$) for *DAB1* in NSCL. The difference in methylation level between NSCL and healthy groups was not statistically significant for *FYN*. Correlation analysis revealed that the degree of methylation in the *DAB1* locus showed a significant negative relationship with *DAB1* expression ($P < 0.01$, $r = -0.6076$). However, no correlation was observed between *FYN* methylation and expression.
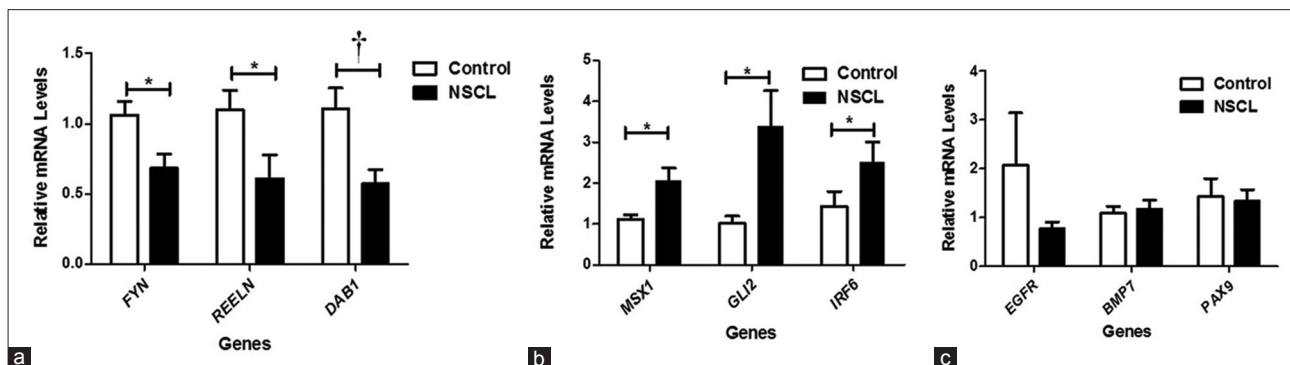
Figure 3: Analysis of the potential relation between mRNA expression and methylation. (a) mRNA levels of *DAB1*, *FYN*, and *REELIN* in NSCL lesion tissues as detected by RT-qPCR were markedly downregulated compared with those in healthy tissues (*DAB1*, $P = 0.0053$; *FYN*, $P = 0.011$; *REELIN*, $P = 0.035$). $*P < 0.05$, $†P < 0.01$ compared with Control group. (b) mRNA levels of *MSX1*, *GLI2*, and *IRF6* in NSCL lesion tissues were markedly upregulated as compared with those in healthy tissues (*MSX1*, $P = 0.013$; *GLI2*, $P = 0.024$; *IRF6*, $P = 0.018$). $*P < 0.05$, compared with Control group. (c) mRNA expression in NSCL lesion tissues of *EGFR*, *BMP7*, *PAX9* shows no significant difference compared with healthy tissues. NSCL: Nonsyndromic cleft lip; *DAB1*: Disabled 1 gene; *MSX1*: Muscle segment homeobox 1; *GLI2*: Glioma-associated oncogene homologue 2; *IRF6*: Interferon regulatory factor 6; *EGFR*: Epidermal growth factor receptor; *BMP7*: Bone morphogenetic protein; *PAX9*: Paired box gene 9; RT-qPCR: Quantitative reverse transcription-polymerase chain reaction. *FYN*: Tyrosine protein kinase fyn.
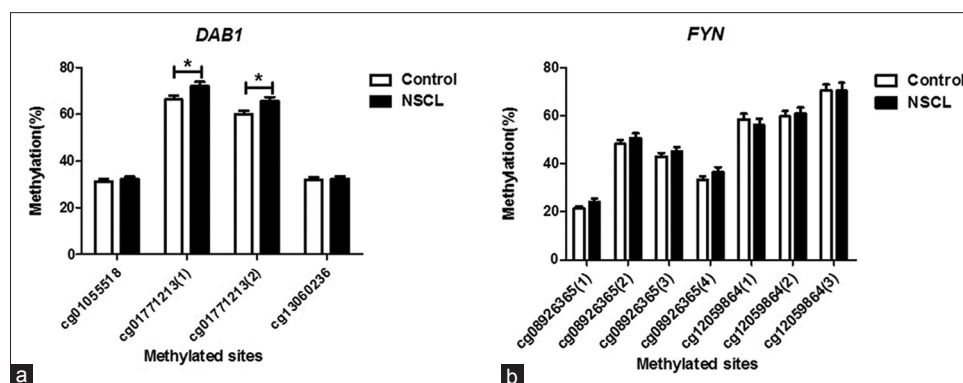

Figure 4: Methylation levels at *DAB1* and *FYN* loci as assessed by pyrosequencing. (a) For *DAB1*, the methylation level at 4 CpG sites was validated by pyrosequencing in 16 NSCL and 15 control tissues. The methylation at two sites covered by the cg01771213 probe was markedly upregulated ($P < 0.05$) in NSCL versus healthy samples. $*P < 0.05$, compared with Control group. (b) Two probes covered 7 CpG sites of FYN. There was no significant difference in methylation level at each CpG site between NSCL and healthy tissues. NSCL: Nonsyndromic cleft lip; *DAB1*: Disabled 1 gene; CpG: Cytosine-phosphoric acid-guanine.

DISCUSSION

Craniofacial formation in the fetus is strictly controlled by complicated gene networks and influenced by environmental factors. The MxP of the first branchial arch and the MNP converge and fuse to form the lips on the 38th day of gestation.[20] Thus, NSCL is the result of the abnormal fusion of the MNP and MxP during the facial developmental process. We detected a total of 4879 aberrant methylation sites in the genes of the NSCL odinopoeia fetus. Among these sites, 3661 were hypermethylated and 1218 were hypomethylated as compared to the methylation levels in healthy lip tissue. The aberrantly methylated loci were mapped to 2849 genes, which were mainly involved in protein site recognition, binding, cellular membrane formation, and other important biological processes. This large number of aberrantly methylated loci might lead to abnormal gene expression and potentially directly or indirectly affect gene expression associated with craniofacial formation. The differential

methylation sites were mainly distributed in CpG islands, and a small portion was located in 0–4-kb regions outside CpG islands. Previous studies have focused on methylation loci within CpG islands because these are mainly located in gene promoters. However, accumulating evidence suggests that certain *cis*-acting elements are located outside of CpG islands, and the methylation level in long, silencing transposons might also affect gene expression.[21] Hence, further studies are needed to investigate the effects of this variety of aberrantly methylated loci located in regions outside or around CpG islands on the etiology of NSCL.

The differentially methylated loci in the 2849 genes mostly were distributed in the gene body, while fewer sites were distributed in the TSS1500 region. Furthermore, it was confirmed that DNA methylation in the gene body is closely associated with gene expression. For example, some CpG islands in the gene body act as a promoter to regulate transcriptional activity during the process of early gamete and embryo formation and lose this function

after the maturation of tissues and organs.[21] A study on X chromosome inactivation revealed that there was a marked discrepancy in the methylation levels of alleles in inactivated X chromosomes compared with those inactivated X chromosomes. In addition, the methylation discrepancy was largely attributed to methylation foci in gene bodies.[21] There is a need to focus more on the roles of localization and distribution of the different methylation loci in NSCL.

Nine candidate genes were tested for expression in the two types of tissues by RT-qPCR. The expression of *DAB1*, *FYN*, and *REELIN* was significantly downregulated in NSCL as compared with healthy tissues. In contrast, the expression of *MSX1*, *GLI2*, and *IRF6* was significantly upregulated in NSCL as compared with healthy tissues. These results may be explained as follows. The effect of the methylation level on gene expression might be tissue specific. Further, it is possible that in some genes, the DNA conformation changes due to locally increased methylation might facilitate the interaction with transcription factors, thus enhancing transcription.

The contribution of common variants to nonsyndromic CPO (NSCPO) has been studied in GWAS. The results suggested that such contribution is limited. In contrast, rare variants may play a substantial role in NSCPO.[22] In the present study, we identified some new genes that were aberrantly expressed due to aberrant methylation that had not been previously reported in the literature. We validated the methylation levels for *DAB1* and *FYN*, whose expression was significantly downregulated, in a larger sample size by pyrosequencing. For *DAB1*, pyrosequencing data confirmed the aberrantly high methylation at two CG loci in the gene in NSCL tissues. However, pyrosequencing revealed no significantly different methylation at the *FYN* locus.

DAB1 is a type of plasmosin with nerve-cell specificity. The *DAB1* gene is located in 1p32-p31. As a key adaptor protein in the REELIN signal pathway, DAB1 is activated upon interaction with the corresponding acceptor at REELIN. This elicits a series of reactions, including the suppression of glycogen synthase, promotion of nerve signal transmission, and adjustment of the growth of nerve cells.[23-25] There is currently no report on the relevance of REELIN signaling and DAB1 in relation to NSCL. The low DAB1 expression resulting from the abnormally high methylation at the gene locus in NSCL lesion tissue might be one of the factors related to the occurrence of NSCL, which will require further study.

One of the limitations of the current study was that only partial population from North China was enrolled. In addition, a limited number of cases were enrolled in this study, which diminished the statistical power of the results.

In conclusion, we detected numerous genome-wide abnormally methylated loci in NSCL lesion tissues. Abnormally methylated loci were distributed mainly in gene bodies and CpG islands, and few were found in TSS1500 and island shores. Abnormal gene expression of the REELIN signaling pathway might be related with NSCL morbidity. Low DAB1 expression resulting from abnormally high methylation in NSCL lesion tissue might be one of the factors underlying the occurrence of NSCL.

Conflicts of interest

There are no conflicts of interest.

REFERENCES

1. Stuppia L, Capogreco M, Marzo G, La Rovere D, Antonucci I, Gatta V, *et al.* Genetics of syndromic and nonsyndromic cleft lip and palate. J Craniofac Surg 2011;22:1722-6. doi: 10.1097/SCS.0b013e31822e5e4d.
2. Rahimov F, Jugessur A, Murray JC. Genetics of nonsyndromic orofacial clefts. Cleft Palate Craniofac J 2012;49:73-91. doi: 10.1597/10-178.
3. Senders CW, Peterson EC, Hendrickx AG, Cukierski MA. Development of the upper lip. Arch Facial Plast Surg 2003;5:16-25. doi: 10.1001/archfaci.5.1.16.
4. Bush JO, Jiang R. Palatogenesis: morphogenetic and molecular mechanisms of secondary palate development. Development 2012;139:231-43. doi: 10.1242/dev.067082.
5. Buchanan EP, Xue AS, Hollier LH Jr. Craniofacial syndromes. Plast Reconstr Surg 2014;134:128e-53e. doi: 10.1097/PRS.0000000000000308.
6. Cielo CM, Marcus CL. Obstructive sleep apnoea in children with craniofacial syndromes. Paediatr Respir Rev 2015;16:189-96. doi: 10.1016/j.prrv.2014.11.003.
7. Grewal J, Carmichael SL, Ma C, Lammer EJ, Shaw GM. Maternal periconceptional smoking and alcohol consumption and risk for select congenital anomalies. Birth Defects Res A Clin Mol Teratol 2008;82:519-26. doi: 10.1002/bdra.20461.
8. Yan J, Song H, Mi N, Jiao X, Hao Y. Nucleotide variants of the NAT2 and EGF61 genes in patients in Northern China with nonsyndromic cleft lip with or without cleft palate. Medicine (Baltimore) 2017;96:e7973. doi: 10.1097/MD.0000000000007973.
9. Hoebel AK, Drichel D, van de Vorst M, Böhmer AC, Sivalingam S, Ishorst N, *et al.* Candidate genes for nonsyndromic cleft palate detected by exome sequencing. J Dent Res 2017;96:1314-21. doi: 10.1177/0022034517722761.
10. Vieira AR. Unraveling human cleft lip and palate research. J Dent Res 2008;87:119-25. doi: 10.1177/154405910808700202.
11. Fan S, Huang K, Ai R, Wang M, Wang W. Predicting CpG methylation levels by integrating infinium HumanMethylation450 BeadChip array data. Genomics 2016;107:132-7. doi: 10.1016/j.ygeno.2016.02.005.
12. McGraw S, Oakes CC, Martel J, Cirio MC, de Zeeuw P, Mak W, *et al.* Loss of DNMT1o disrupts imprinted X chromosome inactivation and accentuates placental defects in females. PLoS Genet 2013;9:e1003873. doi: 10.1371/journal.pgen.1003873.
13. Li E, Bestor TH, Jaenisch R. Targeted mutation of the DNA methyltransferase gene results in embryonic lethality. Cell 1992;69:915-26.
14. Hansen RS, Wijmenga C, Luo P, Stanek AM, Canfield TK, Weemaes CM, *et al*. The DNMT3B DNA methyltransferase gene is

mutated in the ICF immunodeficiency syndrome. Proc Natl Acad Sci U S A 1999;96:14412-7.

15. Martins-Taylor K, Schroeder DI, LaSalle JM, Lalande M, Xu RH. Role of DNMT3B in the regulation of early neural and neural crest specifiers. Epigenetics 2012;7:71-82. doi: 10.4161/epi.7.1.18750.

16. Hatta T, Matsumoto A, Moriyama K, Otani H. Opposite effects of the maternal immune system activated by interleukin-1beta vs. PSK and OK432 on 5-azacytidine-induced birth defects. Congenit Anom (Kyoto) 2003;43:46-56.

17. Kim H, Gordon S, Dionne R. Genome-wide approaches (GWA) in oral and craniofacial diseases research. Oral Dis 2013;19:111-20. doi: 10.1111/j.1601-0825.2012.01962.x.

18. Sandoval J, Heyn H, Moran S, Serra-Musach J, Pujana MA, Bibikova M, et al. Validation of a DNA methylation microarray for 450,000 CpG sites in the human genome. Epigenetics 2011;6:692-702. doi: 10.4161/epi.6.6.16196.

19. Price EM, Peñaherrera MS, Portales-Casamar E, Pavlidis P, Van Allen MI, McFadden DE, et al. Profiling placental and fetal DNA methylation in human neural tube defects. Epigenetics Chromatin 2016;9:6. doi: 10.1186/s13072-016-0054-8.

20. Jiang R, Bush JO, Lidral AC. Development of the upper lip: Morphogenetic and molecular mechanisms. Dev Dyn 2006;235:1152-66. doi: 10.1002/dvdy.20646.

21. Jones PA. Functions of DNA methylation: Islands, start sites, gene bodies and beyond. Nat Rev Genet 2012;13:484-92. doi: 10.1038/nrg3230.

22. Ishorst N, Francheschelli P, Böhmer AC, Khan MF, Heilmann-Heimbach S, Fricker N, et al. Nonsyndromic cleft palate: An association study at GWAS candidate loci in a multiethnic sample. Birth Defects Res 2018;7:e016958. doi: 10.1002/bdr2.1213.

23. Muraoka N, Shum L, Fukumoto S, Nomura T, Ohishi M, Nonaka K, et al. Transforming growth factor-beta3 promotes mesenchymal cell proliferation and angiogenesis mediated by the enhancement of cyclin D1, Flk-1, and CD31 gene expression during CL/Fr mouse lip fusion. Birth Defects Res A Clin Mol Teratol 2005;73:956-65. doi: 10.1002/bdra.20191.

24. Jugessur A, Lie RT, Wilcox AJ, Murray JC, Taylor JA, Saugstad OD, et al. Variants of developmental genes (TGFA, TGFB3, and MSX1) and their associations with orofacial clefts: A case-parent triad analysis. Genet Epidemiol 2003;24:230-9. doi: 10.1002/gepi.10223.

25. Shaw GM, Wasserman CR, Lammer EJ, O'Malley CD, Murray JC, Basart AM, et al. Orofacial clefts, parental cigarette smoking, and transforming growth factor-alpha gene variants. Am J Hum Genet 1996;58:551-61.

非综合症唇裂的甲基化异常位点筛查

摘要

背景： 唇裂病因尚不清楚，是环境因素和遗传因素相互作用的复杂多基因疾病。本研究的目的是利用甲基化芯片技术筛查单纯性唇裂胎儿局部病变组织的甲基化位点，并利用焦磷酸测序技术进行大样本验证初步候选基因。

方法： 搜集了15例引产胎儿正常唇部组织与16例单纯性唇裂引产患儿局部病变组织样本。选择了周龄相匹配的NSCL组和对照组胎儿各3例，取唇部组织提取DNA，采用Illumina公司的Infinium Human Methylation450 BeadChip芯片进行检测。应用R软件的minfi包、GO注释、Pathway代谢通路注释、多样品间表达模式聚类分析等生物信息学方法对差异位点和基因进行功能分析。采用Real-time PCR的方法扩大样本量对筛选出的候选基因在16例患者组和15例对照组中的表达情况进行检测。用焦磷酸测序技术对候选基因位点的甲基化异常进行了验证。

结果： NSCL胎儿的病变组织与正常对照组织相比存在大量的甲基化异常位点，其中高甲基化位点3661个，低甲基化位点1218个。这些甲基化异常位点存在于2849个基因之中。从位点分布的位置来看，在筛选出来的甲基化水平差异位点中，分布于基因本体区、CpG岛的位点占很大比例。另外，也有一些分布在TSS1500区域和岛前区域。REELIN细胞通路中的两个关键转录因子（*DAB1*和*FYN*）在患者组均存在高甲基化的位点。利用Real-time PCR的方法对我们筛选出来的9个候选基因在病变组织中的表达情况进行了检测。结果表明，*DAB1*、*FYN*、*REELIN*基因在NSCL胎儿病变组织中的表达情况与对照组相比，患者组表达下调且有显著差异（P<0.05）。焦磷酸测序验证结果显示，位于*DAB1*基因体区CpG岛的两个CG位点甲基化水平存在显著差异（P<0.05）。即患者组存在高甲基化现象。

结论： NSCL胎儿的病变组织存在大量的甲基化异常位点。NSCL胎儿的病变组织中*DAB1*基因异常的高甲基化导致*DAB1*低表达是NSCL病理改变发生的原因之一。REELIN信号通路基因表达异常可能与NSCL发生有关。